ESS LINAC PLANS FOR COMMISSIONING AND INITIAL OPERATIONS

R. Miyamoto*, M. Eshraqi, M. Muños, ESS, Lund, Sweden

Abstract

Beam commissioning of the proton linac of the European Spallation Source (ESS) is planned to be conducted in 2018 and 2019. At this stage, the last 21 cryomodules are not yet installed and the maximum beam energy and power are 570 MeV and 1.4 MW, with respect to the nominal 2 GeV and 5 MW. The linac will be operated in this condition until the remaining cyromodules are installed in two stages in 2021 and 2022. On top of the common challenges of beam dynamics and machine protection, commissioning of a large scale machine, such as the ESS linac within a relatively short integrated time of less than 40 weeks imposes an additional challenge to the scheduling and planning. This paper lays out the current plans of the ESS linac for its beam commissioning as well as the initial operation.

INTRODUCTION

European Spallation Source (ESS), currently under construction in Lund, Sweden, is a neutron source driven by a proton linac. When the linac reaches its unprecedented design average power of 5 MW, the ESS will the brightest neutron source in the world [1, 2]. It is planned that installation and commissioning of the ESS linac starts in 2017 and the first proton beam is delivered to the target by the end of 2019. The plan as the ESS facility is to start the user program in 2023 and gradually increase the neutron production and operation time towards the design specifications. Commissioning of a large-scale machine, such as the ESS linac, within a relatively short time imposes challenges on many areas including planning and preparations for the beam commissioning (BC). Many efforts have already made for planning of the commissioning from the point of view of the installation [3, 4], radiation permit [5], beam diagnostics devices [6, 7], and control software [8]. In this paper, we review the procedures of the beam commissioning from the point of view of beam physics so that necessary types of lattice tuning and their methods are clarified and prepared prior to the beam commissioning.

ESS LINAC OVERVIEW

High Level Parameters

Table 1 lists the high level parameters of the ESS linac during the nominal operation. The 2 GeV energy, 62.5 mA current, and 4% duty cycle make average power of 5 MW. The long pulse length of 2.86 ms is a requirement from the users and thus fixed during any phase of operation. If the power is needed to be reduced during initial phases of operation, the peak current or and repetition rate is reduced. A high availability of 95% is also a requirement from the users due to the nature of the user program [9].

---

* ryoichi.miyamoto@esss.se

Table 1: High Level Parameters of the ESS Linac

Parameter	Unit	Value
Average beam power	MW	5
Maximum beam energy	GeV	2
Peak beam current	mA	62.5
Beam pulse length	ms	2.86
Beam pulse repetition rate	Hz	14
Duty cycle	%	4
RF frequency	MHz	352.21/704.42
Availability	%	95

Linac Structure

Figure 1 shows a schematic layout of the ESS linac. The initial part of the linac is consist of an ion source (IS); two normal conducting accelerating structures, a radio frequency quadrupole (RFQ) and drift tube linac (DTL); and two beam transports, a low energy beam transport (LEBT) and medium energy beam transport (MEBT). These are referred to as the normal conducting linac (NCL) as a whole. In addition to provide acceleration, functionalities of the NCL includes bunching in the RFQ and manipulations of the beam parameters. Once the beam exits the MEBT, there is no controlled change in the current and pulse length in the downstream section.

Following the NCL, there are three sections with different types of superconducting cavities, spoke cavities, medium-β elliptical cavities, and high-β elliptical cavities. These sections are referred to as SPK, MBL, and HBL for each and Superconducting Linac (SCL) as a whole. As seen in the figure, most of the energy gain is provided by the superconducting cavities in the SCL.

Another beam transport, a high energy beam transport (HEBT), follows the SCL. The HEBT has the same lattice structure as the HBL except the empty slots for the cryomodules, which allow to install additional cryomodules later in cases of contingencies or for an energy upgrade. At the end of the HEBT, there is a dipole for the upward bend and the linac is split into two from this point. When the dipole is off, the beam enters the dump line (DMPL) and is stopped by a tuning dump at the end. When the dipole is on the beam enters the dogleg and is bent back towards the target by another dipole after a 4.5 m elevation. After the second dipole is the final section of the linac and another beam transport, the accelerator-to-target (A2T) section. In the A2T, each pulse is sprayed over a rectangular region on the target surface by fast oscillating (~29 kHz in horizontal plane and ~40 kHz in vertical plane) dipole magnets to reduce the intensity (*rastering* process).

Further details of each section are provided later during the discussion of the commissioning plan for each section.
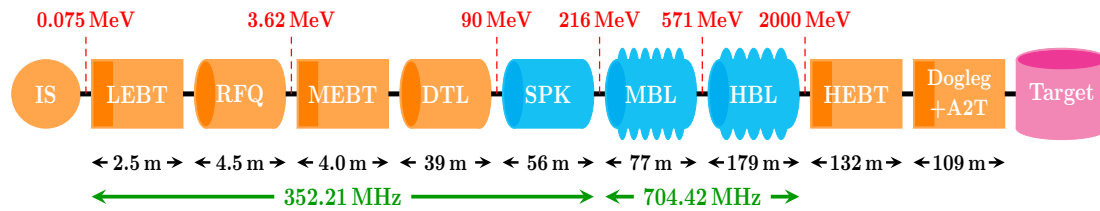
Figure 1: ESS linac schematic layout. Normal conducting structures and beam transports are in orange and superconducting structures are in blue.

BEAM COMMISSIONING OVERVIEW

Plan of the Initial Phase

The installation and commissioning of the ESS linac will be done in stages. On the first stage, starting in 2017, all the components except the cryomodules for the HBL will be installed. The linac will be commissioned at this state, where the maximum energy and average power are 571 MeV and 1.4 MW for each, and operated until the end of 2020. In 2021 and 2022, the cryomodules for the HBL will be installed in two stages, completing installation of all the components. From 2023, performance of the linac will be gradually raised, aiming to achieve the design specifications summarized in Table 1 in around 2025. The focus of this paper is on the initial stage until 2020. The following discusses the schedule and steps of this stage with more details [3–5, 10].

The commissioning of the IS and LEBT has been already started in the lab of the in-kind partner INFN-LNS in Catania, Italy and will be completed, including the beam commissioning, prior to the delivery to the ESS site scheduled in 2017. It is planned to fully test both again in the tunnel before the RFQ is installed.

In late 2018, the RFQ and MEBT will be installed and commissioned together. This means that the beam out of the RFQ must be characterized with diagnostics devices in the MEBT. For some hadron linacs, for instance the CERN LINAC4, the IS, LEBT, and RFQ were commissioned by itself without the following sections and the output beam of each section was characterized with a common movable test bench [11]. The movable bench was also considered for the beam commissioning of the ESS NCL [12] but is not currently in the plan due to the limitations in budget and schedule. By the end of 2018, the first DTL tank out of five will be also installed and commissioned.

In early 2019, DTL tanks 2-4 will be installed and commissioned. Up to this point, the beam will be stopped with a temporary beam stop and temporary shield walls will be placed after the DTL tank 4 to separate the sections under the beam commissioning and the rest and to allow the beam commissioning and other installation works in parallel. The installation of the rest of the sections is scheduled to be completed in mid-2019 and the beam commissioning will be resumed afterward. At this point, the available beam stops are the target, tuning dump, or one of Faraday cups (FCs) used as beam stops, located in the LEBT, MEBT, DTL, SPK, and MBL [6, 7]. Please note that only the target and the FC

in the LEBT can stop the beam with the nominal current and pulse length. The beam commissioning will continue with a low power beam until the beam is safely delivered first to the tuning dump and then to the target. It is aimed to deliver the first beam to the target by the end of 2019 and the the power will be gradually increased towards 1.4 MW afterward.

Beam Modes

In addition to the nominal beam parameters in Table 1, several sets of beam parameters, *beam modes*, are defined to be used during the beam commissioning and general linac tuning [13, 14] (Table 2). The *probe* mode is the lowest power beam, mainly for the very first check of the system and hardware and the beam threading, the process to correct the trajectory and deliver the beam to the designated beam stop. The *fast tuning* and *slow tuning* modes are used to characterized the beam and achieve the desired beam parameters and thus the main types of modes during the beam commissioning. The fast tuning mode is mainly for setting the phases and amplitudes of cavity fields. The slow tuning mode could have a pulse length up 50 µs and this is meant to provide a good quality signal to invasive diagnostics devices, such as FCs and wire scanner (WS) profile monitors. The slow tuning mode will be also used to set the low-level RF (LLRF) feed-backs and feed-forwards for the cavities. The fast and slow tuning beams can be stopped with any of the beam stops.

Once the tuning with low power beams are completed, the next step is to gradually extend the pulse length and verify the beam losses are within the limit. The *long pulse* mode is for this purpose. After the LEBT, this beam can be stopped only with the tuning dump or target. Due to its 12 kW limitation, the tuning dump can stop the long pulse beam with the full current and full pulse length roughly only once per minute. This indicates that verification for high power beams, particularly beams with repetition rate higher than 1 Hz, must be conducted by sending the beam to the target. In addition to the modes listed in the table, another mode to verify the radiation shielding is also under discussion and to be added. Please also note that, to minimize the radiation, further limitations will be applied during the initial phase of the beam commissioning up to the DTL tank 4 [5].

COMMISSIONING OF EACH SECTION

This section provides an overview of the structure and functionalities of each section and discusses its beam com-

Table 2: List of Beam Modes

Type	Destinations	Main usages	Peak current [mA]	Pulse length [μs]	Repetition rate [Hz]
Probe	Any beam stop	Initial check Beam threading	6 - 62.5	≤ 5	≤ 1
Fast tuning	Any beam stop	RF setting	6 - 62.5	≤ 5	≤ 14
Slow tuning	Any beam stop	Invasive measurement LLRF setting	6 - 62.5	≤ 50	≤ 1
Long pulse	Tuning dump Target	Beam loss check Lorentz detuning check	6 - 62.5	≤ 2860	≤ 1/30
Production	Target	Neutron production	6 - 62.5	2860	≤ 14

missioning, focusing on the types of tuning needed for the considered section.

General Strategy

Before going into details of each section, we discuss a general strategy applied to any section. The first step of the beam commissioning is to thread the lowest ~6 mA current probe beam to the designated dump. Polarities of the BPMs, dipole correctors, and quadrupoles should be also checked at this point by producing multiple trajectories and observing the differences (*difference trajectory* method). If the commissioned section includes the RF cavities, the next step is to set the phases and amplitudes of the cavity fields with the phase scan technique, one by one from the first cavity of the section towards the downstream. This process is also done with the probe or fast tuning beam with the lowest current of ~6 mA. The centroid positions in all three planes should have been adjusted at this point but the transverse positions may have to be fine-tuned or readjusted after the transverse matching.

Following the adjustment of the centroid positions is measurement and matching of the Courant-Snyder parameters. The RMS sizes and profiles of the beam are measured with interceptive profile monitors during the beam commissioning and thus the slow tuning beam mode is used for this step. For the sections with a periodic structure (the sections providing acceleration, HEBT, and dogleg), the matching at the interface of two sections is desired. In the MEBT and A2T, adjustments of beam sizes are also required at some locations. Because the Courant-Snyder parameters of the beam depend on the beam current, this step has to be repeated when the current is changed.

After the centroid positions are adjusted and the matching is achieved, we gradually increase the pulse length (long pulse beam mode) and verify the beam losses are within the limit. As the case of the matching, this step also has to be repeated when the current is changed.

IS and LEBT

As already mentioned during the discussion of the plan, the IS and LEBT will be beam commissioned prior to the de-

livery to the ESS site and thus the work after the installation will be verifications of the measurements before the delivery. Nonetheless, as seen in the proposed beam commissioning plan [15], the LEBT has many functionalities and there are a lot of beam parameters to verify. Figure 2 shows a schematic layout of the LEBT. The main components of the LEBT are the two solenoids, chopper, iris, and diagnostics devices.

The diverging beam out of the IS is focused and matched to the RFQ entrance with the two solenoids. In the LEBT, there is a process referred to as *space-charge compensation* (SCC), where the electrons from the ionization of the residual gas, induced by the incoming pulse itself, are trapped within the pulse and reduce the space-charge force. The anticipated level of the SCC is around 95% for the ESS LEBT and thus it has a large impact for the beam focusing. The beam focusing can be verified with measurements of the Courant-Snyder parameters and emittances from the emittance measurement unit (EMU), located between two solenoids. The other commonly used method to optimize the focusing in the LEBT, after the installation of the RFQ, is to scan the solenoids and determine the settings based on the transmission out of the RFQ [16, 17]. The beam parameters out of the LEBT are sensitive to the level of the SCC [17]. If needed, the level of the SCC can be indirectly controlled by adjusting the vacuum level. Each solenoid includes the windings to produce dipole fields of both plane, allowing to correct the transverse centroid positions of the beam. The two non-invasive profile monitors (NPMs) seen in Fig 2 are in fact mainly for measurement of the transverse centroid positions.

During the production of each pulse, the IS is estimated to take a few ms to get stabilized and the beam from this transient period is likely to have wrong parameters. The
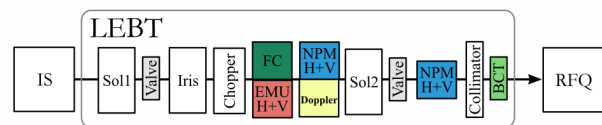

Figure 2: LEBT schematic layout (courtesy of B. Cheymol).

chopper, located between the solenoids, deflects and removes this part of the pulse. This means that, for example when producing a 2.86 ms pulse, the IS outputs a pulse of ~6 ms and approximately the initial half is removed so that the desired 2.86 ms is left. The deflected part of the beam is stopped by the RFQ entrance cone, denoted as "collimator" in Fig 2. Please note that the SCC is induced by the pulse itself and estimated to takes up to ~20 μs to reach to a stable state, meaning that the initial ~20 μs part of the pulse is still likely to have wrong parameters even after using the chopper. This ~20 μs part is removed with the chopper in the MEBT. The function of the chopper can be verified with the beam current transformer (BCT), housed inside the RFQ cone.

The current out of the IS is almost a fixed value. Thus, when producing a lower current beam, the beam is scraped with the iris with a hexagonal shape cross-section, located between the solenoids. The ideal Courant-Snyder parameters at the RFQ entrance are dependent, in fact nonlinear functions, of the peak current [13]. Thus, when the current is reduced with the iris, the solenoids have to be also adjusted accordingly and a well-defined procedure for this process has to be prepared. The reduction of the current is verified also with the BCT inside the RFQ cone.

The beam out of the IS contains not only protons but also other positively charged ions. The design specification is the fraction of the protons is larger than 75%. The Doppler detector allows to verify this fraction based on the difference in the Doppler shifts for different species.

RFQ and MEBT

After the IS and LEBT, the RFQ and MEBT will be beam commissioned together. For the RFQ, the only parameter to adjust is the amplitude of the field to achieve the desired output energy of 3.62 MeV. The output energy is reconstructed from time-of-flight (TOF) measurements with beam position monitors (BPMs) in the MEBT. After setting the amplitude of the field, the transmission should be verified. The efficiency of any RFQ is never perfect and the output beam includes particles not properly accelerated. Figure 3 shows a schematic layout of the MEBT. There is one BCT at the entrance and the other around the middle, behind the chopper dump. These two BCTs are to distinguish the transmissions of the particles with the right energy and the rest. This is based on the result of a study that, for the ESS RFQ, most of the particles with wrong energies have the IS output energy of 75 keV and they do not reach beyond the third quadrupole.

As seen in Figure 3, the MEBT lattice is consist of three buncher cavities, eleven quadrupoles, chopper, and chopper dump. Each quadrupole has additional windings to produce dipole fields of both transverse plane. The beam threading
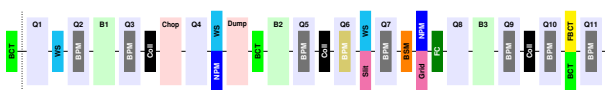
is done with these dipoles and the BPMs installed inside the selected seven quadrupoles. The buncher cavities only provide the focusing in the longitudinal plane and do not change the energy by design. However, in case the output energy of the RFQ is slightly off and cannot be adjusted with the RFQ itself, they are capable of making a small adjustment of energy (the order of tens of keV) as well.

Out of the eleven quadrupoles, the first four are used to adjust the optics of the region with the chopper and it dump. The beam is expanded in both transverse plane at the exit of the chopper dump and the remaining seven quadrupoles are used to refocus the beam and match to the DTL. The MEBT houses three WSs and one EMU, consisting of a slit and grid, for each transverse plane. The measurements from these devices provide enough information to set the transverse optics but a further study should be performed to establish a well-defined process for the real machine. For the longitudinal plane, there is only one profile monitor, *bunch shape monitor* (BSM). Thus, to reconstruct the Courant-Snyder parameters and emittance and achieve the longitudinal matching, measurements with different settings of a buncher cavities are needed.

The function of the chopper will be checked in a later part the MEBT beam commissioning, after the centroid positions and the optics is adjusted. The rise and fall times of the MEBT chopper are on the order of 10 ns. The BPM with a special electronics in the sixth quadrupole and a fast beam current transformer (FBCT) towards the end are capable of measuring currents of single bunches around the leading and trailing edges of a pulse and verifying the function of the chopper. The MEBT includes dual-plane collimators at three locations to remove the halo in the transverse plane. Adjustment of the jaw positions of these collimators is also a process for the later part of the MEBT commissioning. Because the distribution is dependent on the current, this process is also has to be repeated every time when the current and the optics is changed.

DTL

The ESS DTL consists of five tanks. Every other drift tube houses a permanent quadrupole magnet (PMQ), forming a FODO channel, and some of the drift tubes without a PMQ houses a BPM or single plane dipole corrector. Because the transverse focusing is provided by the PMQs, the only parameters to adjust are the phase and amplitude of the field of each tank and dipole correctors.

SCL and HEBT

The three sections of the SCL have a similar lattice structure. One lattice period is consist of one quadrupole doublet and one cryomodule. In-between the doublet quadrupoles, there are a dual-plane dipole corrector, BPM, and space for other types of diagnostics devices (mainly profile monitors). The doublet and these devices in-between form a unit referred to as *linac warm unit* (LWU). Each cryomodule in the SPK houses two spoke cavities and each cryomodule in MBL and HBL houses four elliptical cavities. For each
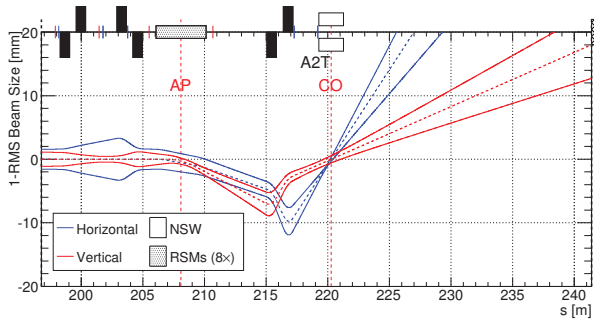

Figure 3: MEBT schematic layout.

Figure 4: A2T schematic layout and RMS beam envelopes inside (courtesy of H. D. Thomsen).

section, the numbers of the lattice periods are 13, 9, and 21, making 62 superconducting cavities in SPK and MBL and 146 in total. Because of this many number of cavities, the major part of the SCL beam commissioning is to set the phases and amplitudes of the fields of all these cavities.

The second, fourth, and fifth LWUs in the SPK and MBL house a WS. These three WSs are to measure the transverse Courant-Snyder parameters and emittances at the initial part of each section and to perform the matching if necessary. The lengths of the LWUs and cryomodules in the MBL and HBL are identical, making the lattice periods of these sections identical. Because of no change in the lattice structure, the transverse matching is not considered at the MBL-HBL interface. The first LWUs in the SPK and MBL house a BSM to measure the longitudinal size and profile of the beam. The reason for the smaller number than the WSs is the difference in cost. As the case of the MEBT, to determine the Courant-Snyder parameters and emittance and and perform the longitudinal matching, multiple measurements have to be made for different settings of upstream cavities.

The HEBT is consist of 16 lattice periods, identical to those in the MBL and HBL. As described in the following, the beam optics of the A2T requires a careful adjustment to meet the requirements from the target. Hence, to provide a properly matched beam to the A2T, the HEBT houses three WSs towards the end. Even if the installation will have been completed through the target, the beam will not be sent to the target until the beam parameters are properly adjusted up to the end of the HEBT. Until then, the will be sent to the tuning dump.

Dogleg and A2T

Similar to the SCL and HEBT, the dogleg is also a focusing channel with quadrupole doublets but with a different period length. It consists of six periods with a vertical phase advance per period of 60 degrees, making it achromatic on the first order [18]. The achromatic condition can be verified by monitoring the vertical position at the first BPM in the A2T while modulating the energy out of the SCL by adjusting the last available cavity.

The target of sets boundaries on the beam parameters on its surface: the intensity has to be within 56 µA/cm² but at

the same 99% of the particles have to be inside a rectangular region of 160×60 cm². The main function of the A2T is to manipulate the beam to meet these requirements. This is achieved by expanding the beam sizes with the optics and also sweeping the centroid position with the raster system. Details on the optics of the A2T and the raster system can be found elsewhere, e.g., [18], but we briefly discuss how to tune the lattice during the beam commissioning in the following. Figure 4 shows a schematic layout of the A2T together with RMS beam sizes of two transverse planes (for the case of the full amplitude of the raster system). The lattice is consist of six quadrupoles (black boxes) and the raster system, consisting of four fast dipole magnets per plane, sitting between the fourth and fifth quadrupoles. The Action Point (AP) is the center of the raster system and the Crossover (CO) is the location of the neutron shield wall, blocking the backscattered particles from the target and thus having an aperture radius of 20 mm, tighter than 60 mm for the upstream part, over a length of ~2 m. The last two quadrupoles between the raster system and CO set the phase advances of the two transverse planes 180 degrees, making the CO a fixed pivot point of the raster motion. There are dual plane corrector dipoles right before and right after the raster system so that the trajectory of the raster motion can be reproduced. By monitoring the position with the BPM at the CO while scanning these two dipole correctors, we can verify the 180 degrees phase advance between the AP and CO. The initial four quadrupoles are setting the beam sizes on the target surface and at the CO. It is planned to have one WS at AP and two imaging systems between the CO and the target. The measurements from these three devices should allow to reconstruct the Courant-Snyder parameters and emittances and thus to achieve the desired beam sizes with the initial four quadrupoles. Once the optics is adjusted, the anticipated maximum extent of the raster system can be verified again with the dipole correctors on the sides of the raster system. The next step is to actually use the raster system and check its function. The two imaging systems between the CO and the target can be used for this.

CONCLUSIONS

Start of the beam commissioning of the ESS linac being approaching, its plan was reviewed from the point of view of beam physics and types of required tuning. It has been identified which lattice components have to be adjusted to achieve the desired value of a given beam parameter. The necessary diagnostics devices for each type of verification and tuning are also checked to be in the plan. For all the types of the tuning, further detailed studies will be conducted to establish well-defined procedures and to understand the limitations.

ACKNOWLEDGMENTS

REFERENCES

[1] M. Lindroos et al., in Proc. of IPAC'16, FRYAA02.

[2] H. Danared, in Proc. of HB'16, MOAM3P30.

[3] E. Tanke and D. McGinnis, "Accelerator Installaon Sequence", ESS Document No. ESS-0037305, 2015.

[4] E. Sargsyan and L. Lari, "Accelerator Installation Plan", ESS Document No. ESS-0055889, 2016.

[5] A. Jansson, "ESS Accelerator First Stage Beam Commissioning Plan", ESS Document No. ESS-0054490, 2016.

[6] S. Molloy, "PBI Taskforce Report", ESS Document No. ESS-0037620, 2015.

[7] A. Jansson et al., in Proc. of IPAC'16, MOPMR020.

[8] Y. I. Levinsen et al., in Proc. of IPAC'16, WEPOY043.

[9] E. Bargalló et al., in Proc. of IPAC'15, MOPTY045.

[10] M. Muñoz, "Warm Linac Beam Commissioning Sequence", ESS Document No. ESS-0043907, 2016.

[11] A. Lombardi et al., in Proc. of LINAC'14, MOIOA02.

[12] B. Cheymol, "Potential Beam Diagnostics for a Movable Test Bench", ESS Document No. ESS-0020683, 2015.

[13] E. Sargsyan and R. Miyamoto, "ESS Linac Beam Modes", ESS Document No. ESS-0037801, 2014.

[14] M. Muñoz, "Description of Modes for ESS Accelerator Operation", ESS Document No. ESS-0038258, 2016.

[15] A. Ponton and B. Cheymod, "Proposal for Off-site Beam Commissioning Sequence of the ESS Proton Source and LEBT", ESS Document No. ESS-0049241, 2016.

[16] Y. I. Levinsen et al., in Proc. of IPAC'15, THPF092.

[17] Y. I. Levinsen et al., in Proc. of IPAC'16, TUPMR020.

[18] H.D. Thomsen and S.P. Møller, in Proc. of IPAC'14, WEPRO073.